

# On how leakage can affect the Star Formation Rate estimation using $H\alpha$ luminosity

M. Relaño<sup>1\*</sup>, R. C. Jr. Kennicutt<sup>2</sup>, J. J. Eldridge<sup>2,3</sup>, J. C. Lee<sup>4</sup>, S. Verley<sup>1</sup>

<sup>1</sup> *Departamento de Física Teórica y del Cosmos, Universidad de Granada, Campus Fuentenueva, Granada, Spain.*

<sup>2</sup> *Institute of Astronomy, University of Cambridge, Madingley Road, Cambridge CB3 0HA.*

<sup>3</sup> *Department of Physics, University of Auckland, Private Bag 92019, Auckland, New Zealand.*

<sup>4</sup> *Space Telescope Science Institute, 3700 San Martin Drive, Baltimore, MD 21218, USA.*

## ABSTRACT

We present observational evidence that leakage of ionising photons from star-forming regions can affect the quantification of the star formation rate (SFR) in galaxies. This effect could partially explain the differences between the SFR estimates using the far ultraviolet (FUV) and the  $H\alpha$  emission. We find that leakage could decrease the  $SFR(H\alpha)/SFR(FUV)$  ratio by up to a 25 per cent. The evidence is based on the observation that the  $SFR(H\alpha)/SFR(FUV)$  ratio is lower for objects showing a shell  $H\alpha$  structure than for regions exhibiting a much more compact morphology. The study has been performed on three object samples: low luminosity dwarf galaxies from the Local Volume Legacy survey and star-forming regions in the Large Magellanic Cloud and the nearby Local Group galaxy M33. For the three samples we find differences ( $1.1 - 1.4\sigma$ ) between the  $SFR(H\alpha)/SFR(FUV)$  for compact and shell objects. Although leakage cannot entirely explain the observed trend of  $SFR(H\alpha)/SFR(FUV)$  ratios for systems with low SFR, we show the mechanism can lead to different SFR estimates when using  $H\alpha$  and FUV luminosities. Therefore, further study is needed to constrain the contribution of leakage to the low  $SFR(H\alpha)/SFR(FUV)$  ratios observed in dwarf galaxies and its impact on the  $H\alpha$  flux as a SFR indicator in such objects.

**Key words:** ISM: HII regions, dust, extinction – galaxies: individual: M33, LMC.

## 1 INTRODUCTION

Measuring the star formation rate (SFR) in galaxies has long been a major field of study in astronomy. Two of the most widely indicators of the star formation are the  $H\alpha$  recombination emission line and the UV non-ionising continuum. The  $H\alpha$  emission is produced by the recombination of the hydrogen ionised by the most massive ( $M \gtrsim 20 M_{\odot}$ ) and short-lived ( $t \lesssim 1\text{--}10$  Myr) stars. The UV emission primarily originates in the photospheres of lower mass ( $M \gtrsim 3 M_{\odot}$ ) and long-lived stars ( $t \lesssim 200$  Myr). Despite the different average timescales in the stellar lifetimes both indicators have been probed to trace well the SFR in galaxies over a range of luminosities and environments (Kennicutt 1998).

The robustness of both indicators has been questioned for objects whose star formation history consists of a set of starburst episodes rather than a constant SFR (Sullivan et al. 2004; Iglesias-Páramo et al. 2004; Boselli et al. 2009; Bell & Kennicutt 2001). Recently, Lee et al. (2009) showed that, in a complete sample of  $\sim 300$  star-forming galaxies within 11 Mpc volume, extinction corrected  $H\alpha$  and far ultraviolet (FUV) emission give consistent SFRs for normal spiral galaxies ( $SFR \approx 1 M_{\odot} \text{ yr}^{-1}$ ). However, for low luminosity dwarf galaxies ( $SFR \approx 0.1 M_{\odot} \text{ yr}^{-1}$ )  $H\alpha$  emission

tends to under predict the SFR relative to the prediction of FUV emission. For galaxies with  $SFR \lesssim 0.003 M_{\odot} \text{ yr}^{-1}$  the ratio of  $SFR(H\alpha)/SFR(FUV)$  is on average lower than expected by a factor of two.

Several explanations have been suggested for explaining this discrepancy (see e.g. Meurer et al. 2009; Lee et al. 2009, for a review): the amount of dust within star-forming regions, star formation history (SFH), porosity of the interstellar medium, stochasticity of the Initial Mass Function (IMF) and IMF variations.

The differences in the SFR derived from  $H\alpha$  and FUV for low star-forming systems are present even when Galactic foreground extinction corrections have been applied to the observed luminosities. For normal spiral galaxies (see also Botticella et al. 2011) the SFR derived from FUV tend to be lower than the one derived using  $H\alpha$  emission, but after accounting for internal attenuation agreement is found using both tracers. However, for low star-forming systems internal attenuation increases the discrepancies between the two SFR estimates (Meurer et al. 2009; Lee et al. 2009).

A departure in the assumption of constant star formation implied in the calibration relations can affect the value of SFR derived from FUV or  $H\alpha$  emission: for a galaxy with systematic star formation bursts the deficiency of ionising short-lived stars relative to the longer-lived lower mass stars emitting in the FUV will produce an  $H\alpha$ -to-FUV ratio lower than expected from a constant

\* E-mail: mrelano@ugr.es

SFH (Sullivan et al. 2004; Iglesias-Páramo et al. 2004). However, to explain the observed variations in the SFR ratio the low star-forming systems must have very intense (a factor of 100) and very long ( $\sim 100$  Myr) bursts of star formation (Iglesias-Páramo et al. 2004). Such bursts of star formation do not seem to occur in these systems based on SFHs reconstructed from resolved stellar populations (Weisz et al. 2008; McQuinn et al. 2009).

Stochastic effects of an invariant IMF (e.g. Cerviño & Luridiana 2004; Corbelli et al. 2009) or variation of the maximum stellar mass that can be formed in a stellar cluster leading to an integrated galactic initial mass function (IGIMF) (Weidner & Kroupa 2005; Pflamm-Altenburg et al. 2009), have been proposed to explain the differences in the observed  $\text{SFR}(\text{H}\alpha)/\text{SFR}(\text{FUV})$  ratios. The assumption of an IGIMF describing the stellar population of the galaxy seems to produce results that explain the observations reasonably well, but it underestimates the  $\text{H}\alpha$  luminosity in systems with low SFR activity (Fumagalli et al. 2011; Weisz et al. 2012). Besides, the variation of an upper mass limit of the IMF is still under discussion, as there is some evidence showing that this variation does not exist (Calzetti et al. 2010). Eldridge (2011) and (Fumagalli et al. 2011) showed that stochastic IMF sampling combined with a cluster mass function and a cluster age distribution can well explain the differences in the  $\text{SFR}(\text{H}\alpha)/\text{SFR}(\text{FUV})$  ratios. Using models of different SFHs and a fully populated IMF, Weisz et al. (2012) compared the predictions of  $\text{SFR}(\text{H}\alpha)$  and  $\text{SFR}(\text{FUV})$  with the observations and were also able to reproduce the decline of the observed  $\text{SFR}(\text{H}\alpha)/\text{SFR}(\text{FUV})$  for lower luminosity systems. However, using the same models, Weisz et al. (2012) were not able to find a strong agreement between the  $\text{H}\alpha$  equivalent width or the UV luminosity modelled distributions and the observed ones.

One of the other plausible explanations for the observed SFR ratio is the leakage of Lyman continuum photons from star-forming regions. In the conversion of  $\text{H}\alpha$  luminosity to star formation, it is assumed that all ionising radiation is absorbed by the neutral hydrogen in the star-forming regions and therefore every Lyman continuum photon will produce an  $\text{H}\alpha$  photon. However, it is known that some of the ionising photons can escape the regions of star formation (e.g. Oey & Kennicutt 1997; Relaño et al. 2002; Eldridge & Relaño 2011) and ionise the diffuse interstellar gas (DIG) in normal galaxies (Zurita et al. 2000, 2002; Wood et al. 2010). Oey et al. (2007) have shown that the fraction of diffuse ionised gas seems to be higher in dwarf galaxies than that observed in normal galaxies. However, whether this translates into a difference in the escape fraction of ionising photons for each type of galaxy remains uncertain (Hanish et al. 2010). If all the ionising photons escaping from the star-forming regions are able to ionise the DIG they should be included when integrating the total  $\text{H}\alpha$  emission from the whole galaxy. Therefore, for a constant SFH, we should not expect discrepancies between the SFR estimates from the total  $\text{H}\alpha$  or FUV luminosity of galaxies. However, if there are ionising photons escaping the galaxy disk or those ionising the DIG are not detected (Melena et al. 2009; Hunter et al. 2010), then we expect to find discrepancies between the SFRs obtained from  $\text{H}\alpha$  and FUV luminosities. Recently, Eldridge (2011) has shown that leakage of ionising photons in combination with pure stochastic IMF sampling better reproduce the observed  $\text{SFR}(\text{H}\alpha)/\text{SFR}(\text{FUV})$  ratio at very low luminosities.

There is some evidence that the H II regions with  $\text{H}\alpha$  shell morphology (normally called bubbles and superbubbles) have in general a higher escape fraction of ionising photons (Oey & Kennicutt 1997), based on the idea that once the shells are formed the ISM can fragment and produces voids of gas where the ionising ra-

diation can escape (Dove et al. 2000). Hoopes & Walterbos (2000) tried to apply this idea to a sample of H II regions in M33 and found no correlation of compact or diffuse star-forming regions with the expected leakage fraction of ionising photons. Recently, Grossi et al. (2010) found that the star-forming regions in M33 associated with younger and lower-mass stellar clusters seem to have higher escape fractions of ionising photons.

In view of the renewed interest in the consistency of  $\text{H}\alpha$  and UV-based SFRs we have undertaken a more comprehensive examination of the possible role of ionising photon leakage from H II regions. We present here observational evidence that even if the fraction of ionising photons escaping from galaxies and star-forming regions is not able to completely explain the observational trends by itself, it should be taken into account when trying to explain the observed phenomenology in combination with other mechanisms. We estimate here that leakage could decrease significantly the  $\text{SFR}(\text{H}\alpha)/\text{SFR}(\text{FUV})$  ratio. Therefore, in order to explain the differences in the quantification of the SFR based on FUV and  $\text{H}\alpha$  luminosities, one should constrain the magnitude of leakage from star-forming regions.

Our study is based on a morphological classification of the H II regions in low surface brightness dwarf galaxies in the Local Volume Legacy (LVL) survey sample (Dale et al. 2009; Lee et al. 2011). Using the  $\text{H}\alpha$  images from the LVL archive, we perform the morphological classification of the galaxies based on the morphology of the most luminous H II regions in each galaxy. The same morphological discrimination is applied on  $\text{H}\alpha$  images of individual regions in the Large Magellanic Cloud (LMC) and the nearby galaxy M33. The most luminous H II regions show  $\text{H}\alpha$  luminosities and SFRs comparable to the low surface brightness dwarf galaxies. Besides, the star formation for these galaxies occur in the form of short-lived burst episodes similar to those in the H II regions (see e.g. Gerola et al. 1980; Weisz et al. 2012), therefore it is reasonable to study and compare both object samples. In Section 2 we explain the data for each sample and the morphological classification we have applied to the objects. In Section 3 we estimate the  $\text{SFR}(\text{H}\alpha)/\text{SFR}(\text{FUV})$  for each object in the samples and show the trends with the  $\text{H}\alpha$  morphology. We analyse the results and show the importance of the leakage effect in the observational trends in Section 4 and the conclusions are presented in Section 5.

## 2 METHODOLOGY

### 2.1 Local Volume Legacy galaxy sample

We classified the LVL galaxies from the Data Release 5<sup>1</sup> (Lee et al. 2009) in terms of morphology using the  $\text{H}\alpha$  images available in the archive. We chose only galaxies with RC3 type T 10 and 11 to avoid grand design spirals. The classification was done visually by one of the authors (MR) in terms of morphology of the H II regions: *compact* are galaxies presenting compact knots (one or several), *mixed* are galaxies presenting compact knots and filamentary structures, and *shells* are galaxies with clear shells (one or several).  $\text{H}\alpha$  images of some examples of each classification are shown in the top row of Fig. 1, while the FUV images of the same objects are shown in the top row of Fig. 2. The integrated  $\text{H}\alpha$  and FUV fluxes for the LVL galaxy sample were presented in Kennicutt et al. (2008) and in Lee et al. (2010), respectively.

<sup>1</sup> <http://irsa.ipac.caltech.edu/data/SPITZER/LVL/>

The comparison of the  $H\alpha$  and FUV SFRs for the galaxy sample was done in Lee et al. (2009) showing that for low luminosity dwarf galaxies  $H\alpha$  luminosity tends to underpredict the SFR relative to the FUV luminosity. The trend is seen not only for Galactic extinction corrected SFRs but also when internal extinctions were applied. The  $H\alpha$  extinction was derived using the Balmer decrement while the extinction in the FUV was obtained using the total infrared (TIR) to FUV flux ratio and applying models from Buat et al. (2005). For those objects with no available TIR emission estimates scaling relations were used to derive the FUV extinction. Besides, scaling relations were used when Balmer decrements or TIR/FUV ratios were not available (see Lee et al. 2009).

## 2.2 Sample of star-forming regions in M33

We selected a sample of star-forming regions in the nearby galaxy M33. This galaxy is a particularly suitable object for this study because its distance (840 kpc; Freedman et al. 1991) allowed us to observe the H II regions as individual objects and to perform a morphological classification of the sample. Besides, the large number of star-forming regions in the disk of M33 allowed us to create a significant statistical sample of objects. Some clear shells have been observed in several wavelength ranges from the optical to the Far Infrared (FIR) with the recent observations from Herschel (Kramer et al. 2010; Verley et al. 2010). An example is shown in the lower-right corner of Fig. 1, this shell is also clearly revealed in the FIR bands from Herschel observations (Verley et al. 2010) and will be studied in detail in Relaño et al. (2012, in prep.).

We used the continuum-subtracted  $H\alpha$  image of M33 from Hoopes & Walterbos (2000) to select our sample. The angular resolution of this image,  $5''$ , corresponding to a linear scale of  $\sim 20$  pc, is good enough to identify the H II region sample. The H II region selection was done visually by one of the authors (MR), as the aim was to find a set of relatively isolated objects with a clear morphology which facilitates the classification (see also Relaño et al. 2012, in prep.). The morphological classification was done using the wide-field KPNO mosaic  $H\alpha$  images from the Local Group Galaxy Survey (LGGS) collaboration (Massey et al. 2006). These  $H\alpha$  images provide a much better spatial resolution ( $\sim 0.8$  arcsec, corresponding to  $\sim 4$  pc) allowing a more accurate morphological classification. Our final sample consists of 117 objects. We applied the same criteria for the morphological classification as described in section 2.1 and found 10 compact regions, 46 mixed regions and 61 regions with shell morphology.

We performed photometry in the FUV,  $H\alpha$ ,  $24\mu\text{m}$  and  $8\mu\text{m}$  bands using individual apertures for each H II region. The FUV image was taken from the GALEX (Martin et al. 2005; de Paz et al. 2007) data archive. The angular resolution for this image was  $\sim 4''$ . The  $8\mu\text{m}$  and  $24\mu\text{m}$  emissions were obtained from the IRAC and MIPS (*Spitzer*) images with  $\sim 3''$  and  $6''$  resolution, respectively. The data reduction of the *Spitzer* images is explained in Verley et al. (2007). As the images were used to obtain the TIR luminosity of the objects, we needed to eliminate the stellar contribution in these bands. We used the IRAC- $3.6\mu\text{m}$  image and followed the relation proposed by Helou et al. (2004) for this purpose. Finally, all the images were smoothed to a common  $6''$  resolution (the  $24\mu\text{m}$  band resolution, which is the lowest one for the images of M33 used in this study) and registered to the same pixel size as the  $H\alpha$  image from Hoopes & Walterbos (2000).

The  $H\alpha$  photometry was performed on the Hoopes & Walterbos image, as the  $H\alpha$  image of the LGGS collaboration presented some saturated zones in the brightest part of the most luminous

H II regions. The FUV and  $H\alpha$  fluxes were corrected for Galactic extinction using  $E(B - V) = 0.07$  (van den Bergh 2000) and Cardelli et al. (1989) extinction law. The internal  $H\alpha$  extinction for each region was obtained using the  $H\alpha$  and  $24\mu\text{m}$  fluxes and assuming that the absorbed  $H\alpha$  luminosity in the region scales with the  $24\mu\text{m}$  luminosity with a factor of  $a = 0.031$  (Kennicutt et al. 2007). FUV extinction was obtained using the empirical relation between the ratio of the TIR to FUV luminosities and the UV spectral index  $\beta$  following the formalism given in Calzetti (2001). The TIR emission was obtained from the linear combination of  $8\mu\text{m}$  and  $24\mu\text{m}$  fluxes given in Table 1 in Boquien et al. (2010) corresponding to regions with  $45''$  aperture size. We compare the  $H\alpha$  and FUV extinctions in the left panel of Fig. 3. For most of the H II regions the relation between both extinctions agrees well with the expected relation ( $A(\text{FUV}) = 1.8 \times A(\text{H}\alpha)$ ) from Calzetti's reddening curve. The values of the FUV extinction are within the range obtained by Verley et al. (2009).

## 2.3 H II region sample in the Large Magellanic Cloud

Our H II region selection for the LMC was determined by the sample presented in Bell et al. (2002), which represents a subsample of isolated regions from Caplan & Deharveng (1986). Bell et al. (2002) presented the fluxes at  $H\alpha$  and  $1500\text{\AA}$  for a set of H II regions in the LMC within a diameter aperture of  $4.9'$ , corresponding to 65 pc at the distance of LMC (45.9 kpc; Fitzpatrick et al. 2002). We performed the morphological classification using the LMC  $H\alpha$  image from Kennicutt & Hodge (1986) with an angular resolution image of  $\sim 7$  arcsec. The classification was done visually by one of the authors (MR). We applied the same criteria as those for the LVL and the M33 sample and catalogued the H II region sample. We found 20, 16 and 16 compact, mixed and shell regions, respectively.

Foreground Galactic extinction correction was applied to both  $H\alpha$  and FUV ( $1500\text{\AA}$ ) fluxes using the Galactic reddening  $E(B - V) = 0.06$  given in Bell et al. (2002). These authors also estimate the internal  $H\alpha$  and FUV extinction for each region. The former is based on the Balmer decrement and the latter on the TIR/FUV ratio with the calibrations derived in Gordon et al. (2000). We compare both extinctions in the right panel of Fig. 3. Most of the regions show higher values of FUV extinctions than those derived using Calzetti's extinction curve. However, as we study here the H II regions from M33 and LMC in a separated way the fact that we apply different extinction laws for the two samples does not affect the final results of this paper.

## 3 RESULTS

In Fig. 4 we reproduce figure 5 from Lee et al. (2009) using a colour-code for each classified galaxy: *compact* are blue, *mixed* are green and red are *shells*. In general, the galaxies classified as mixed are slightly more luminous than the compact or shells:  $\langle \log L(H\alpha/\text{erg s}^{-1}) \rangle = 38.8 \pm 0.2$ ,  $\langle \log L(H\alpha/\text{erg s}^{-1}) \rangle = 39.3 \pm 0.2$ ,  $\langle \log L(H\alpha/\text{erg s}^{-1}) \rangle = 38.7 \pm 0.2$  for compact, mixed, and shells, respectively. This is expected as the mixed galaxies are formed by several intense knots of star formation intertwined with some diffuse emission. The mean value for the  $\log(\text{SFR}(H\alpha)/\text{SFR}(\text{FUV}))$  ratio in galaxies classified as mixed is higher than for the compact and shells, the shells having the lowest ratio:  $\langle \log(\text{SFR}(H\alpha)/\text{SFR}(\text{FUV})) \rangle$  is  $-0.32 \pm 0.06$ ,  $-0.22 \pm 0.06$  and  $-0.43 \pm 0.07$  for compact, mixed and shells, respectively. In an

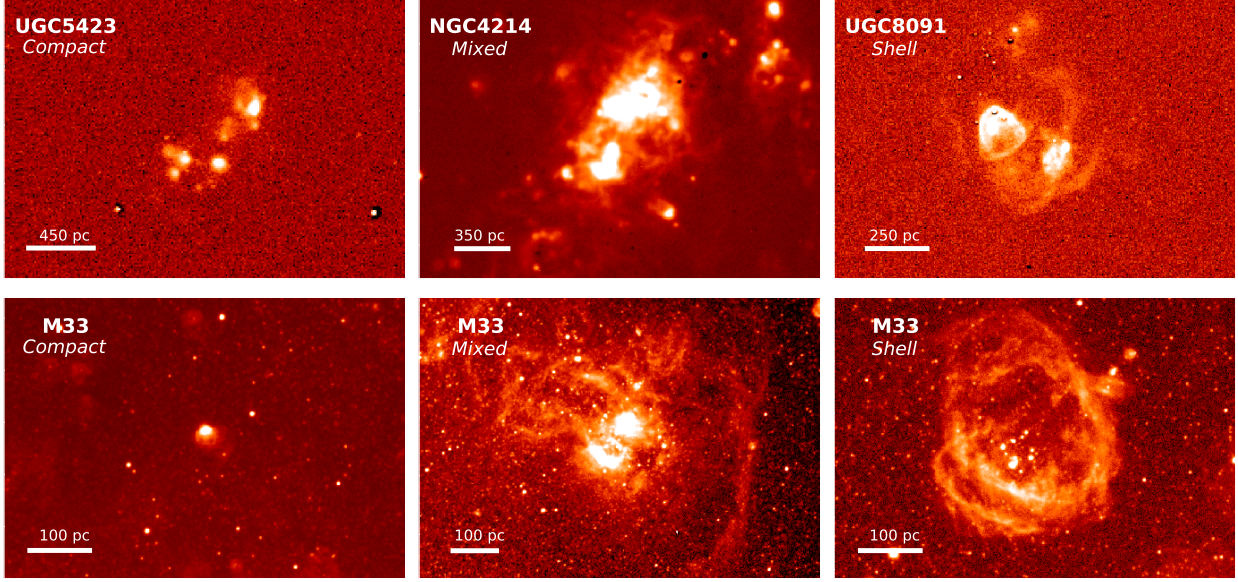


**Figure 1.**  $H\alpha$  images for examples of compact, mixed and shell objects: galaxies in the LVL sample are shown in the top row, while the star-forming regions in M33 are shown in the bottom row.

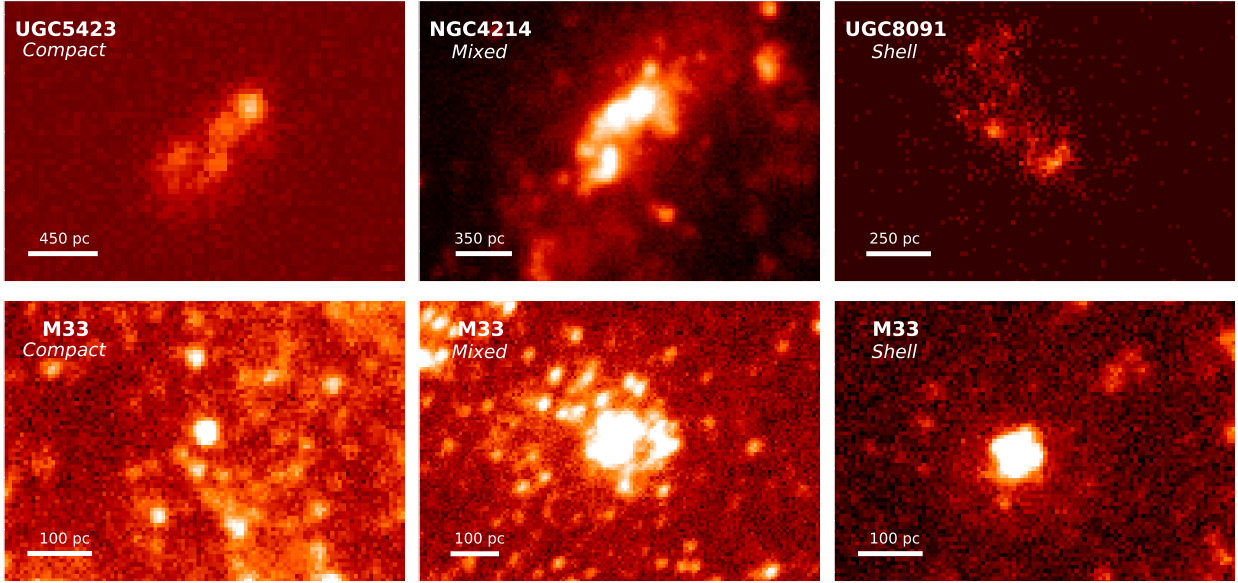


**Figure 2.** FUV images of the same objects as those shown in Fig. 1: galaxies in the LVL sample are shown at the top, while the star-forming regions in M33 are shown in the bottom row.

attempt to quantify this trend we have performed a linear fit to the data in Fig. 4 for each classification. The fits are shown in the figure with the corresponding colour line for each morphology: blue for compacts, green for mixed and red for shells. The results of the fit are presented in Table 1. The linear fit for the shell morphology has the steepest slope, while the mixed show the shallowest one. We will discuss these results in section 4.

We used the  $H\alpha$  and FUV extinction derived in the previous section to correct the observed  $H\alpha$  and FUV fluxes of the H II regions in M33. Then, we converted them into SFRs using the relations given in Kennicutt (1998). These relations assume a

constant SFRs over  $\approx 100$  Myr and are suitable for galaxies rather than for H II regions caused by short-lived bursts of star formation. However, we still apply these relations in order to compare the results with the LVL sample. Since we are using the ratio between the two SFR calibrators our conclusions will not change if we use other calibrations more suitable for H II regions. In Fig. 5 we present the logarithm of  $\text{SFR}(H\alpha)/\text{SFR}(\text{FUV})$  as a function of the logarithmic  $H\alpha$  luminosity for the H II regions in M33. The colour code is the same as in Fig. 4. The mixed regions are in general more luminous than the compact regions and the shells: mean values for the logarithmic  $H\alpha$  luminosity for each class are:

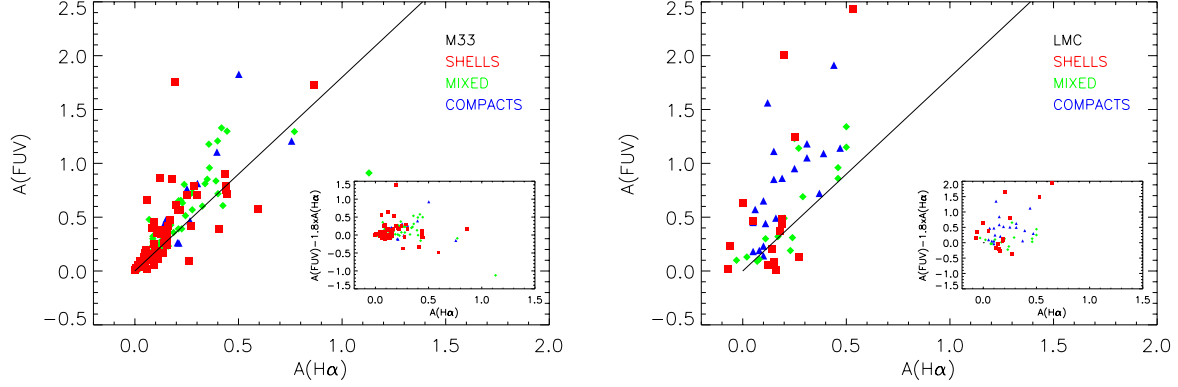


**Figure 3.** Left: FUV extinction versus  $H\alpha$  extinction for the H II region sample in M33. The continuous line represents the relation  $A(\text{FUV}) = 1.8 \times A(H\alpha)$  derived using the Calzetti’s reddening curve. The  $H\alpha$  extinction was obtained using the  $H\alpha / 24\mu\text{m}$  ratio. Right: Same figure but for the H II region sample in LMC. The  $H\alpha$  extinction was obtained using the  $H\alpha / H\beta$  emission line ratio. In the lower-right corner of each plot we show the difference between  $A(\text{FUV})$  and the values expected following Calzetti’s reddening curve.

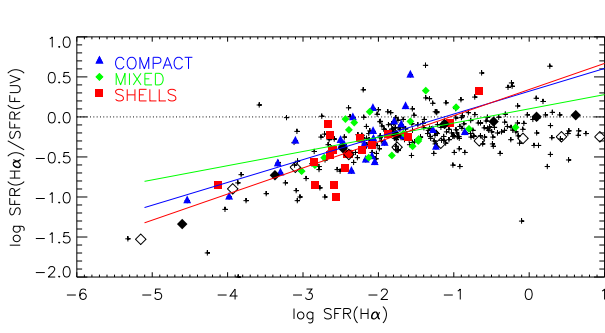


**Figure 4.** Logarithm of the  $\text{SFR}(H\alpha)/\text{SFR}(\text{FUV})$  versus logarithm of the  $\text{SFR}(H\alpha)$  for the LVL galaxy sample (from Fig. 5 in Lee et al. 2009) with colour-code in terms of morphology. Blue: compact galaxies, green: galaxies catalogued as mixed, and red: galaxies with  $H\alpha$  shell morphology. A least-square linear fit is shown for each morphology. The open and compact black diamonds correspond to the standard and minimal models of the IGIMF from Pflamm-Altenburg et al. (2009).

$\langle \log L(H\alpha/\text{erg s}^{-1}) \rangle = 37.6 \pm 0.1$ ,  $\langle \log L(H\alpha/\text{erg s}^{-1}) \rangle = 38.1 \pm 0.2$  and  $\langle \log L(H\alpha/\text{erg s}^{-1}) \rangle = 37.6 \pm 0.1$  for compact, mixed and shells, respectively. The mean values of the SFR ratios,  $\langle \log(\text{SFR}(H\alpha)/\text{SFR}(\text{FUV})) \rangle$ , are  $0.07 \pm 0.06$ ,  $0.03 \pm 0.03$  and,  $-0.03 \pm 0.03$  for compact, mixed, and shells, respectively. The difference between  $\langle \log(\text{SFR}(H\alpha)/\text{SFR}(\text{FUV})) \rangle$  for compact and shells is  $0.10 \pm 0.07$ , a marginal difference of  $1.4\sigma$ . The continuous lines in Fig. 5 show the linear fit to the data in each classification (see Table 1 for fitting coefficients).

$H\alpha$  and FUV fluxes for the regions in the LMC have been corrected from the extinction derived in Bell et al. (2002) and SFR calibrations have been applied to derived the corresponding SFRs using the relations in Kennicutt (1998). The results are shown in Fig. 6, as well as the linear fits for each classification (see Table 1 for fitting coefficients). For this sample, there is also a marginal separation between the  $\log(\text{SFR}(H\alpha)/\text{SFR}(\text{FUV}))$  ratio for compact and for shell regions:  $\langle \log(\text{SFR}(H\alpha)/\text{SFR}(\text{FUV})) \rangle$  are  $0.27 \pm 0.06$ ,  $0.19 \pm 0.08$  and  $0.15 \pm 0.07$  for compact, mixed and shells, re-

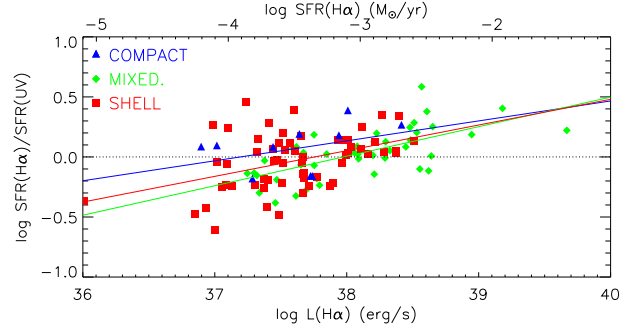


**Figure 5.** Logarithm of  $\text{SFR}(H\alpha)/\text{SFR}(\text{FUV})$  versus logarithm of the  $H\alpha$  luminosity for the H II regions in M33 sample. Extinction corrections to  $H\alpha$  and to FUV luminosities have been applied. A least-square linear fit is shown for each morphology classification.

spectively. The difference in the mean values between compacts and shells is  $0.12 \pm 0.09$ , a  $1.3\sigma$  difference.

We have not combined the H II regions of M 33 and LMC because the samples were not created using the same procedure. For M 33 we used the  $H\alpha$  image from Hoopes & Walterbos (2000) and identified those isolated H II regions with clear morphology. For LMC, we did not create the sample, we rather performed the morphological classification of a set of H II regions previously identified with the purpose of studying the Balmer extinction in each region (see Caplan & Deharveng 1986). Therefore, the H II regions in LMC are biased to the most luminous ones emitting at  $H\alpha$  and  $H\beta$ . This bias can produce systematic differences in the  $H\alpha$  luminosity ranges between M 33 and LMC samples that can affect the comparison when the combined sample is studied as a single set.

We quantify the distribution of the  $\log(\text{SFR}(H\alpha)/\text{SFR}(\text{FUV}))$  ratios using histograms for the LVL, M 33 and LMC samples (Fig. 7, upper, mid, and bottom panels, respectively). We only show the compact and shell classifications to clarify the results. The bins in  $\log(\text{SFR}(H\alpha)/\text{SFR}(\text{FUV}))$  are 0.2 dex for the three sets. The separation between compacts and shells for the LVL, M 33, and LMC samples are  $0.11 \pm 0.10$ ,  $0.10 \pm 0.07$ , and  $0.12 \pm 0.09$ . In the

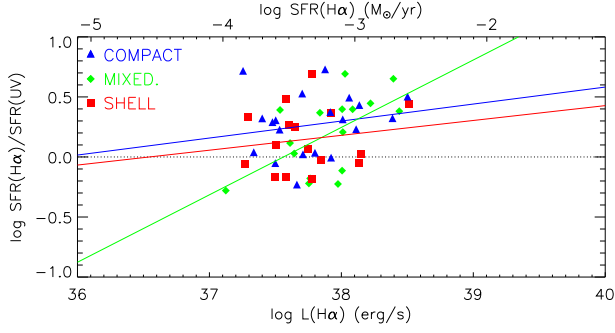


**Figure 6.** Logarithm of  $\text{SFR}(\text{H}\alpha)/\text{SFR}(\text{FUV})$  versus logarithm of the  $\text{H}\alpha$  luminosity for the H II regions in LMC sample. Extinction corrections derived from Bell et al. (2002) have been applied. A least-square linear fit is shown for each sample.

**Table 1.** Linear fits for the data:  $\log(\text{SFR}(\text{H}\alpha)/\text{SFR}(\text{FUV})) = a \times \log(L(\text{H}\alpha)) + b$ .

Sample	Type	$a$	$b$	correl. coeff.
LVL	compact	$0.28 \pm 0.06$	$0.3 \pm 0.1$	0.70
LVL	mixed	$0.18 \pm 0.08$	$0.1 \pm 0.2$	0.50
LVL	shells	$0.33 \pm 0.07$	$0.3 \pm 0.2$	0.73
M 33	compact	$0.2 \pm 0.1$	$-6 \pm 5$	0.40
M 33	mixed	$0.25 \pm 0.04$	$-9 \pm 2$	0.67
M 33	shells	$0.21 \pm 0.06$	$-8 \pm 2$	0.43
LMC	compact	$0.1 \pm 0.2$	$-5 \pm 6$	0.19
LMC	mixed	$0.6 \pm 0.2$	$-21 \pm 8$	0.58
LMC	shells	$0.1 \pm 0.2$	$-5 \pm 8$	0.15

three samples we find marginal separations,  $\sim 1.1 - 1.4\sigma$ , for the compact and shell distributions.

#### 4 DISCUSSION

In the previous section we have presented the trends of the  $\text{SFR}(\text{H}\alpha)/\text{SFR}(\text{FUV})$  for each data sample: the dwarf galaxies with moderate SFR from the LVL sample and the set of H II regions in the nearby M 33 and LMC. Most of the objects in the three samples are in the range of low SFR regime,  $-5 < \log \text{SFR}(\text{H}\alpha)/(\text{M}_{\odot}\text{yr}^{-1}) < -1$ . In each sample the mean values of  $\log(\text{SFR}(\text{H}\alpha)/\text{SFR}(\text{FUV}))$  are lower for the objects catalogued as shells than for the rest of the objects, either mixed or compact regions. For the LVL sample we find a difference in the  $\log(\text{SFR}(\text{H}\alpha)/\text{SFR}(\text{FUV}))$  for compact and shells of  $0.11 \pm 0.10$  and for M 33 and LMC samples we find differences of  $0.10 \pm 0.07$  and  $0.12 \pm 0.09$ .

If the shell morphology of star-forming regions favours the existence of zones of low density gas via holes or fragmentation of the shell walls, and the ionising photons are indeed more likely to leak the star-forming regions between the fragments, then the difference in  $\log(\text{SFR}(\text{H}\alpha)/\text{SFR}(\text{FUV}))$  between compact and shells could be due to the leakage of ionising photons.

It is interesting to note that Hoopes & Walterbos (2000) did not find a correlation between the diffuse and ring H II regions

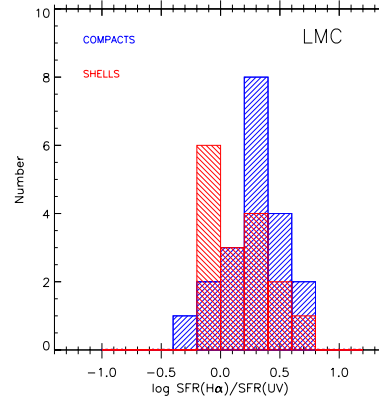
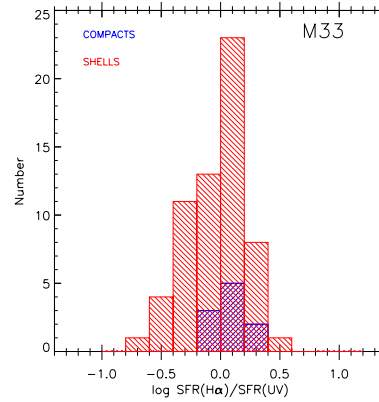
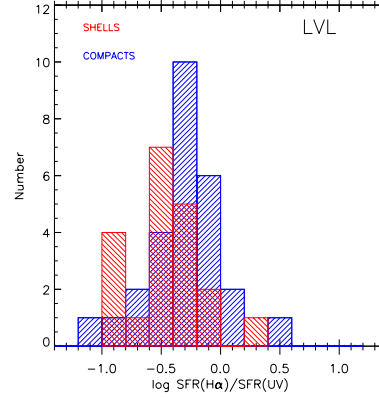


**Figure 7.** Histograms of the  $\log(\text{SFR}(\text{H}\alpha)/\text{SFR}(\text{FUV}))$  for the three samples. All data are extinction corrected. Red histograms are for shells and blue for compact regions.

in M 33 and the fraction of ionising photons escaping the regions. However, these authors are restricted to regions in M 33 for which they were able to study the stellar content. These H II regions have low luminosity (only a few are more luminous than  $10^{38} \text{ erg s}^{-1}$  after extinction correction has been applied) and they represent a small fraction of the H II region population in M 33 (see fig. 1 of Hoopes & Walterbos 2000). In order to infer firm conclusions about whether leakage is more important in shells and ring-



like regions than in compact objects, a detailed study of the stellar content of H II regions with different morphology would be needed.

Assuming that compact regions are able to absorb all the ionising radiation –which would be a strong case, as a compact region with a low filling factor would be able to leak radiation through the zones between clumps (see Giammanco et al. 2004, 2005)– and the shells leak all the ionising radiation coming from the stellar cluster; then we could say that the difference between the  $\log(\text{SFR}(\text{H}\alpha)/\text{SFR}(\text{FUV}))$  of compact and shells would be entirely due to a leakage effect. The maximum observed difference of 0.12 between the compact and shell regions translates into a factor of 0.76 between the  $\text{SFR}(\text{H}\alpha)/\text{SFR}(\text{FUV})$  ratio. Therefore, we can say that leakage could change the  $\text{SFR}(\text{H}\alpha)/\text{SFR}(\text{FUV})$  ratio between 0 to  $\sim 25$  per cent.

We can compare our results with those expected from model stellar populations. We use the single-star stellar populations of Eldridge & Stanway (2009) that assume the H II region stellar population is described by an instantaneous burst with a Chabrier IMF (Chabrier 2003). These predict a  $\log(\text{L}(\text{H}\alpha)/\text{L}(\text{FUV}))$  of the order of 0.4 for an H II region 4 Myr old. However, for our observed H II regions,  $\log(\text{L}(\text{H}\alpha)/\text{L}(\text{FUV})) \approx 0.01$ –0.02, much lower than the model ratios. Therefore, leakage of ionising photons is expected if the age of the H II regions are  $\approx 4$  Myr. Indeed, for NGC 604 and for the set of H II regions from Oey & Kennicutt (1997) included in our LMC sample we observe  $\log(\text{L}(\text{H}\alpha)/\text{L}(\text{FUV})) \approx 0.01$ –0.02, consistent with a leakage fraction ( $\sim 0$ –50 per cent) estimated for these regions (Eldridge & Relaño 2011, for NGC 604, and Oey & Kennicutt 1997 for the LMC H II regions).

The models only predict ratios of the order of 0.01 at an age of 10 Myr. It is unlikely for compact H II regions emitting at  $\text{H}\alpha$  to be this old, but shell-like H II regions are expected to have ages greater than 4 Myr and the assumption of no leakage could be plausible. Recently, Whitmore et al. (2011) have shown evidence of the relation between the region morphology and the age of the central stellar cluster: very young (a few Myr) clusters show the  $\text{H}\alpha$  emission of the ionised gas coincident with the cluster stars, for slightly older clusters ( $\approx 5$  Myr) the gas emission is located in small shell structures around the stars, and in still older clusters ( $\approx 5$ –10 Myr) the  $\text{H}\alpha$  emission shows even larger shell structures. They also show that if no  $\text{H}\alpha$  emission is associated with the cluster then this is generally older than  $\approx 10$  Myr. Following this study our sample of objects would be younger than 10 Myr, as they still exhibit  $\text{H}\alpha$  emission associated with the stellar clusters. Moreover, assuming a standard shell expansion velocity of  $60 \text{ km s}^{-1}$  the radii of the shells at  $t = 10$  Myr would be  $\approx 600 \text{ pc}$  (Relaño & Beckman 2005; Verley et al. 2010). Most of the observed H II regions in our sample are smaller, therefore their age must also be less than 10 Myrs.

We have run models to describe the behaviour of the  $\log(\text{SFR}(\text{H}\alpha)/\text{SFR}(\text{FUV}))$  ratio as a function of age. For a  $10^5 M_{\odot}$  stellar cluster, typical of the most luminous H II regions, the  $\log(\text{SFR}(\text{H}\alpha)/\text{SFR}(\text{FUV}))$  ratio decreases by a factor of more than one order of magnitude between the young (2–3 Myr) and the more evolved (5–8 Myr) H II regions. For a coeval stellar population we would then expect a separation between compact and shells of one order of magnitude if age is the only responsible to explain the differences in  $\log(\text{SFR}(\text{H}\alpha)/\text{SFR}(\text{FUV}))$ .

Other mechanism that can decrease the number of ionising photons is the absorption of Lyman continuum photons by the dust inside the regions (McKee & Williams 1997; Hirashita et al. 2003; Iglesias-Páramo et al. 2004). This mechanism will decrease the  $\text{SFR}(\text{H}\alpha)/\text{SFR}(\text{FUV})$  ratio, as less ionising photons will be able to ionise the hydrogen. We would then expect that regions with lower

$\text{SFR}(\text{H}\alpha)/\text{SFR}(\text{FUV})$  would have higher dust fractions; namely, shell regions would have higher fractions of dust than compact regions. This seems not plausible as shells normally have swept up the gas and dust and do not show in general emission at  $24 \mu\text{m}$  (see Verley et al. 2010).

Despite of the intrinsic difficulties in quantifying the escape fraction of ionising photons from star forming regions, we show here that this mechanism has an effect in the observed trends for  $\text{SFR}(\text{H}\alpha)/\text{SFR}(\text{FUV})$ . Leakage mechanism, in combination with possible variations of the IMF: via stochasticity (Cervino & Luridiana 2004), random sampled IMF (Corbelli et al. 2009) or assuming an IGIMF (Pflamm-Altenburg et al. 2009), might well explain the differences in the  $\text{SFR}(\text{H}\alpha)/\text{SFR}(\text{FUV})$  for star-forming objects.

## 5 SUMMARY AND CONCLUSIONS

We have studied the SFR for a sample of H II regions in M33, LMC, and a set of dwarf galaxies in the LVL sample. We have classified them in compact, mixed, and shell regions and analysed the  $\text{SFR}(\text{H}\alpha)/\text{SFR}(\text{FUV})$  ratio for the three morphology types. For M33 and LMC samples we obtained differences of  $0.10 \pm 0.07$  and  $0.12 \pm 0.09$  in the  $\langle \log(\text{SFR}(\text{H}\alpha)/\text{SFR}(\text{FUV})) \rangle$  between compact and shell regions, a separation of  $\sim 1.4 - 1.3\sigma$ . For the LVL sample we found a smaller difference,  $\langle \log(\text{SFR}(\text{H}\alpha)/\text{SFR}(\text{FUV})) \rangle = -0.32 \pm 0.06$  for compacts and  $\langle \log(\text{SFR}(\text{H}\alpha)/\text{SFR}(\text{FUV})) \rangle = -0.43 \pm 0.07$  for shells, corresponding to a difference of  $0.11 \pm 0.10$ . The maximum observed difference of 0.12 between the compact and shell regions translates into a factor of 0.76 between the  $\text{SFR}(\text{H}\alpha)/\text{SFR}(\text{FUV})$  ratio.

We present here observational evidence that the escape of ionising photons from individual star-forming regions in M33, LMC, and a sample of dwarf galaxies might account for up to a 25 per cent decrease in the  $\text{SFR}(\text{H}\alpha)/\text{SFR}(\text{FUV})$ . Rather than performing a detailed quantification of the leakage fraction of ionising photons we show here that this mechanism should be considered when trying to explain the lower than expected  $\text{SFR}(\text{H}\alpha)/\text{SFR}(\text{FUV})$  for low star-forming objects. It will probably be a combination of different mechanisms: leakage, variations of IMF, SFH, and age effects, which might finally explain the decrease of the  $\text{SFR}(\text{H}\alpha)/\text{SFR}(\text{FUV})$  ratio for low luminosity systems.

## 6 ACKNOWLEDGMENTS

We would like to thank C. Hao, B. Johnson and J. E. Beckman for their useful discussions. MR has been supported by a Marie Curie Intra European Fellowship within the 7th European Community Framework Programme and part of this research has been supported by the ERG HER-SFR from the EC. This work was partially supported by a Junta de Andalucía Grant FQM108, a Spanish MEC Grant AYA-2007-67625-C02-02, and Juan de la Cierva fellowship Program.

## REFERENCES

- Bell E. F., Gordon K. D., Kennicutt R. C., et al., 2002, *ApJ*, 565, 994
- Bell E. F., Kennicutt R. C., 2001, *ApJ*, 548, 681
- Boquien M., Bendo G., Calzetti D., et al., 2010, *ApJ*, 713, 626
- Boselli A., Boissier S., Cortese L., et al., 2009, *ApJ*, 706, 1527

- Botticella M. T., Smartt S. J., Jr. R. C. K., et al., 2011, arXiv, astro-ph.CO
- Buat V., Iglesias-Páramo J., Seibert M., et al., 2005, ApJ, 619, L51
- Calzetti D., 2001, PASP, 113, 1449
- Calzetti D., Chandar R., Lee J. C., et al., 2010, ApJ, 719, L158
- Caplan J., Deharveng L., 1986, Astronomy and Astrophysics (ISSN 0004-6361), 155, 297
- Cardelli J. A., Clayton G. C., Mathis J. S., 1989, ApJ, 345, 245
- Cerviño M., Luridiana V., 2004, A&A, 413, 145
- Chabrier G., 2003, PASP, 115, 763
- Corbelli E., Verley S., Elmegreen B. G., et al., 2009, A&A, 495, 479
- Dale D. A., Cohen S. A., Johnson L. C., et al., 2009, ApJ, 703, 517
- de Paz A. G., Boissier S., Madore B. F., et al., 2007, ApJS, 173, 185
- Dove J. B., Shull J. M., Ferrara A., 2000, ApJ, 531, 846
- Eldridge J. J., 2011, arXiv, 1106, 4311
- Eldridge J. J., Relaño M., 2011, MNRAS, 411, 235
- Eldridge J. J., Stanway E. R., 2009, MNRAS, 400, 1019
- Fitzpatrick E. L., Ribas I., Guinan E. F., et al., 2002, ApJ, 564, 260
- Freedman W. L., Wilson C. D., Madore B. F., 1991, ApJ, 372, 455
- Fumagalli M., da Silva R. L., Krumholz M. R., 2011, arXiv, astro-ph.CO
- Gerola H., Seiden P. E., Schulman L. S., 1980, ApJ, 242, 517
- Giammanco C., Beckman J. E., Cedrés B., 2005, A&A, 438, 599
- Giammanco C., Beckman J. E., Zurita A., et al., 2004, A&A, 424, 877
- Gordon K. D., Clayton G. C., Witt A. N., et al., 2000, ApJ, 533, 236
- Grossi M., Corbelli E., Giovanardi C., et al., 2010, A&A, 521, 41
- Hanish D. J., Oey M. S., Rigby J. R., et al., 2010, ApJ, 725, 2029
- Hirashita H., Buat V., Inoue A. K., 2003, A&A, 410, 83
- Hoopes C. G., Walterbos R. A. M., 2000, ApJ, 541, 597
- Hunter D. A., Elmegreen B. G., Ludka B. C., 2010, AJ, 139, 447
- Iglesias-Páramo J., Boselli A., Gavazzi G., et al., 2004, A&A, 421, 887
- Kennicutt R. C., 1998, ARA&A, 36, 189
- Kennicutt R. C., Calzetti D., Walter F., et al., 2007, ApJ, 671, 333
- Kennicutt R. C., Hodge P. W., 1986, ApJ, 306, 130
- Kennicutt R. C., Lee J. C., Funes S. J., et al., 2008, ApJS, 178, 247
- Kramer C., Buchbender C., Xilouris E. M., et al., 2010, A&A, 518, L67
- Lee J. C., de Paz A. G., Kennicutt R. C., et al., 2010, ApJS, 192, 6
- Lee J. C., de Paz A. G., Kennicutt R. C., et al., 2011, The Astrophysical Journal Supplement, 192, 6
- Lee J. C., de Paz A. G., Tremonti C., et al., 2009, ApJ, 706, 599
- McKee C. F., Williams J. P., 1997, Astrophysical Journal v.476, 476, 144
- Mcquinn K. B. W., Skillman E. D., Cannon J. M., et al., 2009, ApJ, 695, 561
- Martin D. C., Fanson J., Schiminovich D., et al., 2005, ApJ, 619, L1
- Massey P., Olsen K. A. G., Hodge P. W., et al., 2006, AJ, 131, 2478
- Melena N. W., Elmegreen B. G., Hunter D. A., et al., 2009, AJ, 138, 1203
- Meurer G. R., Wong O. I., Kim J. H., et al., 2009, ApJ, 695, 765
- Oey M. S., Kennicutt R. C., 1997, MNRAS, 291, 827
- Oey M. S., Meurer G. R., Yelda S., et al., 2007, ApJ, 661, 801
- Pflamm-Altenburg J., Weidner C., Kroupa P., 2009, MNRAS, 395, 394
- Relaño M., Beckman J. E., 2005, A&A, 430, 911
- Relaño M., et al., 2012, in preparation
- Relaño M., Peimbert M., Beckman J., 2002, ApJ, 564, 704
- Sullivan M., Treyer M. A., Ellis R. S., et al., 2004, MNRAS, 350, 21
- van den Bergh S., 2000, The galaxies of the Local Group
- Verley S., Corbelli E., Giovanardi C., et al., 2009, A&A, 493, 453
- Verley S., Hunt L. K., Corbelli E., et al., 2007, A&A, 476, 1161
- Verley S., Relaño M., Kramer C., et al., 2010, A&A, 518, L68
- Weidner C., Kroupa P., 2005, ApJ, 625, 754
- Weisz D. R., Johnson B. D., Johnson L. C., et al., 2012, ApJ, 744, 44
- Weisz D. R., Skillman E. D., Cannon J. M., et al., 2008, ApJ, 689, 160
- Whitmore B. C., Chandar R., Kim H., et al., 2011, ApJ, 729, 78
- Wood K., Hill A. S., Joung M. R., et al., 2010, ApJ, 721, 1397
- Zurita A., Beckman J. E., Rozas M., et al., 2002, A&A, 386, 801
- Zurita A., Rozas M., Beckman J. E., 2000, A&A, 363, 9